

**MOLDOVA STATE UNIVERSITY
DOCTORAL SCHOOL OF NATURAL SCIENCES**

Consortium: Moldova State University, Institute for Development of the Information Society,
State University "Bogdan Petriceicu Hasdeu" from Cahul

As a manuscript
C.Z.U: 537.222.22:621.315.592:620.97(043.2)

LUNGU ION

**PHYSICS OF CdS/ZnTe HETEROSTRUCTURES IN
PHOTOVOLTAIC APPLICATIONS**

134.01 Physics and Materials Technology

Abstract of the PhD thesis

CHISINAU, 2024

The thesis was developed in the "Organic/Inorganic Materials in Optoelectronics" laboratory at the Moldova State University, Doctoral School of Natural Sciences.

Scientific leader-

POTLOG Tamara PhD in physical and mathematical sciences, Associate professor, Moldova State University

Composition of the Doctoral Commission:

CULIUC Leonid Academician, PhD Habil. in physical and mathematical sciences, University Professor, Institute of Applied Physics, Moldova State University - **president of commission**

POTLOG Tamara PhD in physical and mathematical sciences, Associate professor, Moldova State University - **scientific leader**

NICORICI Valentina PhD in physical and mathematical sciences, Associate professor, Moldova State University - **reviewer**

LUCA Dumitru Doctor, Professor Emeritus, Alexandru Ioan Cuza University in Iasi, Romania - **reviewer**

TROFIM Viorel PhD Habil. in Engineering, University Professor, Technical University of Moldova - **reviewer**

The thesis will defend on 08.10.2024, at 15:00 in the meeting of the doctoral Commission for the public defense of the PhD thesis of the Doctoral School of Natural Sciences, USM. The seat - Moldova State University (<http://www.usm.md>), M. Kogălniceanu street 65 A, study block no.3, hall 332, MD-2009, Chisinau, Moldova

The PhD thesis and abstract can be consulted in the National Library of the Republic of Moldova, Central Scientific Library "Andrei Lupan" (Institute), Central Library of the State University of Moldova (MD 2009, mun. Chisinau, 60 Alexei Mateevici street), on ANACEC web page (<http://www.cnaa.md>), and on the USM web site (<http://www.usm.md>).

The abstract was sent on ” 23 ”August 2024

President of commission


Academician, PhD Habil. in physical and mathematical sciences,


(signature)

CULIUC Leonid

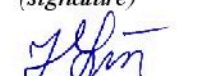
Scientific leader

PhD in physical and mathematical sciences


(signature)

POTLOG Tamara

Author:


(signature)

LUNGU Ion

SUMMARY

SUMMARY.....	3
CONCEPTUAL GUIDLINES OF THE RESEARCH.....	4
THESIS CONTENT.....	7
GENERAL CONCLUSIONS.....	24
RECOMMENDATION.....	26
BIBLIOGRAPHY.....	27
LIST OF AUTHOR'S PUBLICATIONS ON THESIS TOPIC.....	28
ADNOTARE.....	32
ANNOTATION.....	33
АННОТАЦИЯ.....	34

CONCEPTUAL GUIDELINES OF THE RESEARCH

Actuality and importance of the topic

Currently, approximately 95% of the global photovoltaic device market is based on silicon technology. However, silicon is not considered the ideal material for solar panels as it does not efficiently absorb light. Researchers are exploring alternatives such as thin-film and perovskite solar cell technologies [1]. Perovskites have already achieved efficiencies like silicon, with solar energy conversion rates more than 25%, but they remain unstable, a problem that has yet to be resolved. A promising approach involves tandem photovoltaic cells, which combine silicon with perovskites, potentially achieving efficiencies over 30% [2]. Additionally, thin films based on A^2B^6 compounds have garnered attention due to their ability to form high-performance semiconductor devices. CdTe-based photovoltaic cells have already been commercially implemented and exhibit better energy efficiency and degradation rates than silicon-based technologies [3]. Over 30 GW based CdTe modules are installed at global level, with commercial module efficiencies reaching up to 18.6% and laboratory devices more than 22% [4], making this one of the fastest-growing and most promising thin-film technologies. Further efficiency improvements for these devices heavily depend on enhancing the open-circuit voltage (V_{oc}) and fill factor (FF) through innovations in materials, fabrication methods, and device layer design. Another area of interest in photovoltaics is oxygen-doped ZnTe layers, which form highly mismatched alloys (HMAs) with significantly fundamental properties by replacing a small fraction of host atoms with elements of different electronegativity [5], because of the interaction between localized oxygen states and electrons in the conduction band of ZnTe forms an intermediate band. The approach of using intermediate band (IB) materials offers an attractive prospect for achieving high efficiency in a single heterojunction device. To successfully develop IB photovoltaic cells based on ZnTe:O thin films, it is crucial to develop a method for the epitaxial growth of high-quality ZnTe:O thin films. Various research groups have already produced such layers using methods like molecular beam epitaxy or pulsed laser deposition. The physical properties of binary semiconductor compounds with an intermediate band are currently insufficiently studied, hindering progress in their practical application in real devices. Therefore, challenges remain regarding the structural design and photophysical properties of electronic devices using CdS as a "window" layer and ZnTe with an intermediate band. Therefore, optimizing the design, studying their electrical and optical characteristics, and investigating key aspects related to photovoltaic devices based on these compounds are current objectives. Enhancing device efficiency can only

be achieved by optimizing the physical properties of each individual layer and the overall design of the photovoltaic cell.

The aim of this research is to analyze the potential of using CdS/ZnTe HJs in photovoltaic applications through numerical simulation with SCAPS-1D, develop the technology for achieving an intermediate band in the ZnTe absorber layer by incorporating oxygen into the lattice, and investigate their electrical and photoelectrical properties.

The main research objectives proposed in this work are:

1. Numerical simulation using the SCAPS-1D software to predict the performance of the CdS/ZnTe photovoltaic device and identify general principles for optimizing its photovoltaic parameters.

2. Optimize the technologies for obtaining of ZnO and CdS thin films with controlled composition and morphology using spray pyrolysis and close space sublimation methods.

3. Characterize the optical and structural properties of ZnO and CdS thin films, used as transparent electrodes and optical windows, respectively, in the photovoltaic device made later.

4. Develop the technology for obtaining ZnTe:O thin films, identifying the optimal annealing regime in an oxygen environment to form the intermediate band.

5. Establish the correlation between the technological regime (T_s , T_{sub} , t) and the oxygen concentration in ZnTe:O thin films by studying their composition, optical characteristics, and photoluminescence.

6. Estimate the main functional parameters and analyze the characteristics of the CdS/ZnTe:O HJ based on certain physicochemical parameters of the absorber layer obtaining technology and the design of the back contact.

7. Determine the charge carrier transport mechanism through the CdS/ZnTe:O heterojunction.

Research Hypothesis

○ The conversion efficiency numerically simulated with the SCAPS-1D software of HJ CdS/ZnTe is dependent on the parameters of the component layers, for example, for $d_{ZnTe}=1,0 \mu\text{m}$, $d_{CdS}=5 \text{ nm}$, $d_{ZnO}=20 \text{ nm}$, $E_{g(CdS)}=2,4 \text{ eV}$, $E_{g(ZnO)}=3,3 \text{ eV}$, $\Phi_{(Ag)}=4,7 \text{ eV}$, the following photovoltaic parameters were obtained: $V_{oc}=0.89 \text{ V}$, $J_{sc}=25.9 \text{ mA/cm}^2$, $FF=72.6\%$, $\eta=16.78\%$.

○ The optimal technological conditions for obtaining ZnTe thin films using the CSS method are: substrate temperature $320 \text{ }^\circ\text{C} - 360 \text{ }^\circ\text{C}$; source temperature $360 \text{ }^\circ\text{C} - 600 \text{ }^\circ\text{C}$; deposition time 6 minutes. Annealing in an oxygen environment at a treatment temperature of $400 \text{ }^\circ\text{C}$ for 1 hour highlights the formation of the intermediate band.

- The formation of the intermediate band in ZnTe thin films is confirmed by: EDX analysis indicating the presence of oxygen, with its amount decreasing with source temperature from 5.88% (for $T_s = 560$ °C) to 0.68% (for $T_s = 600$ °C); reduction in the crystalline lattice parameter of the oxygen-rich absorber layer; and the presence of a broad band located at 1.6 eV – 2.0 eV in the photoluminescence spectra.
- The conductivity mechanism in the CdS/ZnTe:O HJ at low frequencies (10^2 Hz - 10^4 Hz) is predominantly ionic conductivity, while at high frequencies (10^5 Hz - 10^6 Hz) it exhibits interface polarization conductivity.
- The realized CdS/ZnTe HJs have a $V_{oc}=0.84$ V, $J_{sc}=0.25$ mA/cm², the conversion efficiency of solar energy into electrical energy of 0.13% under integral light illumination of 100 mW/cm². The internal quantum efficiency indicates a slightly higher value of more than 0.5 in the wavelength range of 490-590 nm.

Research methodology synthesis and justification of chosen methods

The scientific problem elucidated in this thesis involves the development of an intermediate band photovoltaic device by optimizing the technology for obtaining thin films of binary compounds with controlled composition, morphology, optical and electrical properties, and studying the electrical and photoelectric properties of these devices. To achieve ZnTe:O thin films with an intermediate band, the CSS method was used along with thermal treatment in an oxygen environment at 400 °C for 1 hour, for ZnO was used the spray pyrolysis method. The thin film structures were investigated through X-ray diffraction, while morphology and chemical composition were analyzed using scanning electron microscopy and energy-dispersive X-ray spectroscopy. Surface roughness was assessed using atomic force microscopy. Transmittance, reflectance, and absorbance were measured via UV-Vis spectroscopy. Photoluminescence spectra highlighted the intermediate band in the ZnTe layer, indicating tellurium substitution with oxygen and the formation of the O_{Te} center. Photovoltaic parameters such as V_{OC} , J_{SC} , R_s , R_{sh} , FF , and η were determined by measuring the J-V characteristics under AM1.5 conditions. Electrical properties were studied through J-V characteristics in the dark, C-V characteristics at different frequencies and temperatures (220 - 350 K), and impedance spectroscopy as a function of temperature and frequency (10^3 - 10^6 Hz).

THESIS CONTENT

In the **Introduction**, the relevance of the research topic is justified, the aim and objectives of the thesis, the scientific research methodology, the novelty of the results obtained, the scientific problem addressed, the theoretical and practical significance of the work, the main scientific results proposed for support, the approval of the results and the structure of the work are presented.

Chapter 1 is dedicated to the bibliographic analysis of research on materials from the class of binary compounds (ZnO, CdS, ZnTe) and the design of photovoltaic devices based on these materials. This chapter presents general aspects and a synthesis of the most recent scientific publications regarding the structure and the structural, morphological, topological, electrical, and optical properties of these materials. Additionally, the specialized literature on the design of photovoltaic devices based on these materials is analyzed, describing the charge transport mechanisms through the heterojunctions formed by the mentioned thin films. In the context of photovoltaic device design, numerical simulation methods allow the inclusion of important physical effects that could not be considered experimentally. To enhance the efficiency of the devices up to the Shockley-Queisser limit, various simulation programs such as PC-1D, AMPS-1D, ADEPT-F, and SCAPS-1D have been developed, aiding in the optimization of the design and comparison with other competing proposals. In this thesis, the SCAPS-1D program was used.

Chapter 2 presents the technology for obtaining thin films of ZnTe, CdS, ZnO, and the heterojunctions based on these materials. The influence of deposition technological parameters, such as the substrate and source temperature, on the morphology, chemical composition, surface topology, and crystalline structure of ZnTe and CdS thin films obtained by the close space sublimation method is discussed. ZnTe and CdS films were deposited on borosilicate glass substrates without using an additional gaseous transport agent. To determine the optimal growth conditions for ZnTe thin films, two sets of samples were obtained: in the first set, the substrate temperature (T_{sub}) was varied while maintaining a constant source temperature (T_S), and in the second set, T_S was varied while keeping T_{sub} constant. The deposition duration was the same for both sets. The method of obtaining ZnO thin films by spray pyrolysis is also described, considering the molar concentration of the precursor solution, the flow rate of the carrier gas, and the substrate temperature. The carrier gases, purified argon, and oxygen, influence the deposition process and the properties of the resulting thin films by providing a controlled environment and chemically interacting with the precursor solution to modify the composition and properties of the films. Aluminum doping is used to introduce controlled impurities into the ZnO lattice, altering the material's optoelectronic properties. To investigate the effect of Al doping on ZnO films, two sets

of samples were obtained in different gaseous environments: one in O₂ and the other in Ar. Both sets of samples were doped with different concentrations of Al, ranging from 0-5%, in the initial precursor solution. The technology for obtaining CdS/ZnTe heterojunctions involves several critical steps essential for their efficiency: depositing the front contact (such as ZnO, SnO₂, ITO, ITO/ZnO) by spray pyrolysis; depositing the "window" layer (CdS) by evaporation in CSS; depositing the absorber layer (ZnTe) by evaporation in CSS and thermal treatment in an oxygen environment; depositing the Sb/Te buffer layer at the back contact by thermal evaporation in a vacuum or PEDOT:PSS by spin-coating; and depositing the ohmic back contact by vacuum thermal evaporation.

Chapter 3 is dedicated to the study of the influence of deposition technological parameters on the morphology, chemical composition, crystalline structure, and optical properties of each component of the CdS/ZnTe heterojunction, namely, ZnO, CdS, and ZnTe.

AFM analysis shows that the surface roughness parameters of ZnO layers obtained in an O₂ environment indicate higher values ($R_{MS}=60.96$ nm) compared to the parameters of undoped ZnO layers obtained in an Ar environment ($R_{MS}=29.48$ nm), as shown in Fig. 1. XRD analysis indicates that all ZnO thin films have a polycrystalline structure, highlighting the diffraction planes (0 0 0 2), (1 0 0 0), and (1 0 0 1), which correspond to the hexagonal wurtzite structure of ZnO, with the c-axis perpendicular to the substrate surface. The nanostructured ZnO thin films exhibit high transmittance (80-85%) in both deposition environments. For ZnO thin films obtained in an O₂ environment, the bandgap value (E_g) is approximately 3.24 ± 0.02 eV. For films obtained in an Ar environment, E_g varies from 3.22 eV to 3.27 eV.

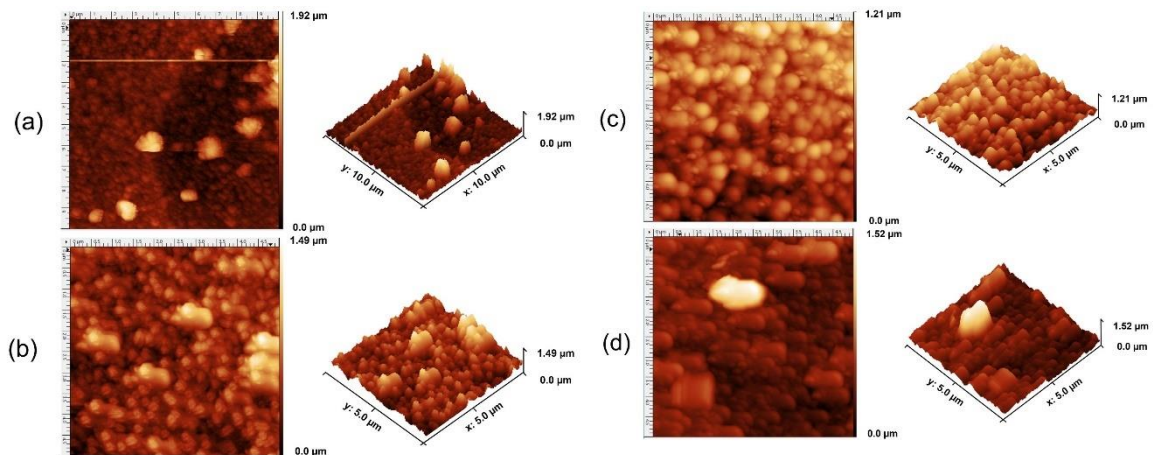


Fig. 1. AFM images of undoped ZnO thin films obtained in an O₂ environment (a); undoped ZnO thin films obtained in an Ar environment (b); Al-doped ZnO thin films obtained in an Ar environment (c); ZnO thin films doped with 2% Al obtained in an Ar environment (d) and treated in vacuum at 420 °C.

The XRD study results in Fig. 2.a of the CdS thin films show that, regardless of the thermal treatment environment, they are polycrystalline and belong to the hexagonal crystallographic system. The average crystallite size reaches its maximum value when thermal treatment is performed in a vacuum. The calculated bandgap value (E_g) from the reflectance (R) and transmittance (T) spectra indicates a value of 2.40 ± 0.02 eV (Fig. 2.b).

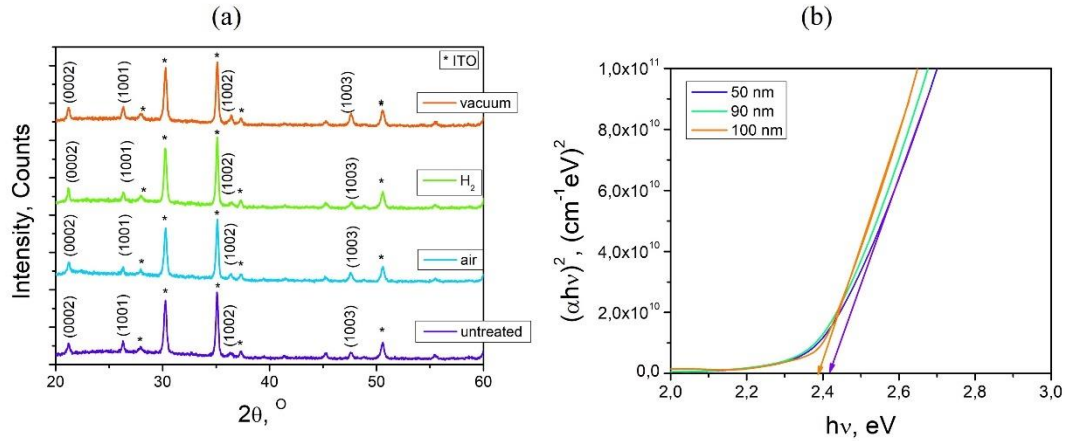


Fig. 2. XRD diffraction patterns (a) and the dependence of $(\alpha hv)^2 = f(hv)$ of the CdS thin films (b)

A more detailed study was conducted on the ZnTe:O absorber layer. These layers were obtained using the CSS method. The deposition conditions of the ZnTe thin films were modified according to the data presented in Table 1.

Table 1. Technological parameters used in the obtaining of ZnTe thin films, along with their specific resistivity.

T_s , °C	T_{sub} , °C	t_{dep} , min	R , $10^9 \Omega$	ρ , $\Omega \cdot \text{cm}$
580	320	6	27,06	13,5
	330		2,83	1,4
	340		2,41	1,2
	350		2,90	1,5
	360		0,88	0,4
560	340		1,62	0,8
570			4,50	2,3
580			2,41	1,2
590			30,44	15,2
600			4,87	2,4

Subsequently, these two sets of ZnTe films obtained under different technological conditions of T_{sub} and T_s were transferred to a furnace (Fig. 3) for treatment in an O_2 environment. The entire treatment process lasted 1 hour at a temperature of 400 °C, with an oxygen flow rate set at 5 ml/min.

EDX analysis confirms the presence of an excess of tellurium (Te) in both sets of samples as per Table 2. It is observed that the amount of Te increases with the increase in the source temperature (T_s), while the percentage of oxygen decreases. This observation can be explained by

the possible incorporation of oxygen as a substitutional impurity at the tellurium site (O_{Te}) during the growth process of ZnTe:O thin films.

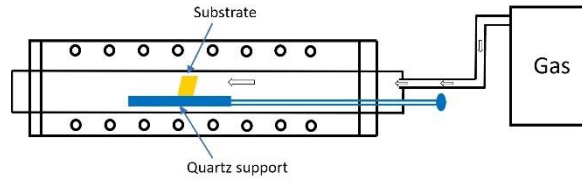


Fig. 3. Annealing in an O_2 environment

This incorporation of oxygen into the ZnTe lattice can result in iso-electronic states, where oxygen atoms substitute for tellurium atoms in the lattice, thereby maintaining the compound's charge balance. This phenomenon can influence the chemical composition of ZnTe:O thin films, causing an excess of tellurium and a decrease in the percentage of oxygen detected in EDX spectra.

Table 2. EDX analysis of ZnTe:O thin films

	$T, ^\circ\text{C}$	Element, %		
		O	Zn	Te
T_{sub}	320	2,09	47,81	50,10
	340	1,55	48,67	49,78
	360	4,49	48,16	49,35
T_s	560	5,88	47,80	46,32
	580	3,05	47,49	49,46
	600	0,69	49,17	50,14

In Fig. 4, XRD diffraction patterns of ZnTe thin films after annealing in an O_2 environment are presented, as a function of T_{sub} (a) and T_s . All samples exhibit a polycrystalline structure with preferential orientation along the [1 1 1] direction.

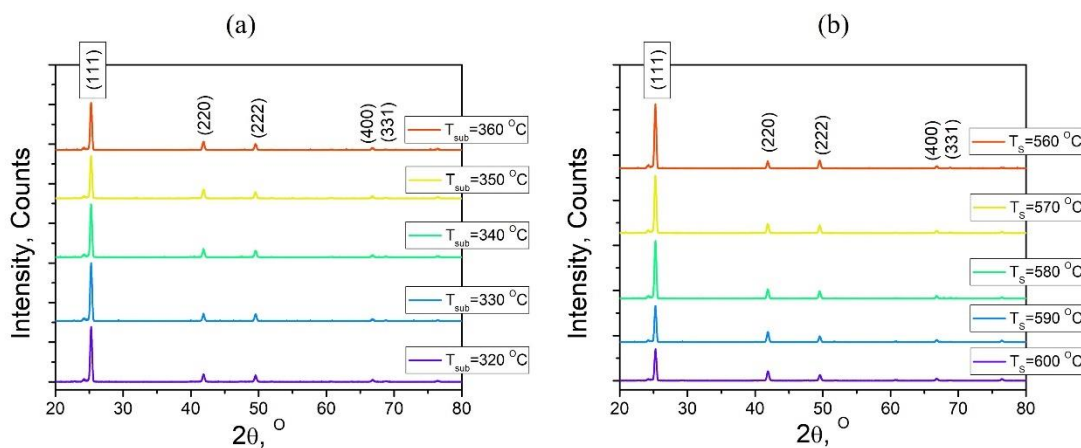


Fig. 4. XRD diffraction patterns of ZnTe:O thin films as a function of T_{sub} (a) and T_s (b).

All diffraction peaks match well with the reference data ICDD #15-0746 and #96-900-8859 [6]. Estimated microstructural parameters from the XRD diffraction patterns are presented in Table 3. It is observed that the intensities of the ZnTe diffraction peaks improve with increasing

source temperature from 560 °C to 600 °C. This can be explained by the higher deposition temperature producing greater surface kinetic energies.

Table 3. Microstructural parameters of ZnTe:O thin films

T_S , °C	T_{sub} , °C	2θ , °	I , Counts	a , Å	d , Å	D , nm	ϵ_{st}
580	320	25,27	1384	6,101	3,523	32,3	$1,12 \cdot 10^{-3}$
	330	25,27	1464	6,100	3,524	33,2	$1,14 \cdot 10^{-3}$
	340	25,27	1338	6,102	3,524	28,5	$0,64 \cdot 10^{-3}$
	350	25,26	1073	6,101	3,524	27,2	$0,47 \cdot 10^{-3}$
	360	25,26	1193	6,102	3,524	28,9	$0,61 \cdot 10^{-3}$
560	340	25,28	708	6,099	3,523	27,7	$0,75 \cdot 10^{-3}$
570		25,27	823	6,101	3,524	28,1	$0,57 \cdot 10^{-3}$
580		25,26	1297	6,102	3,524	27,2	$0,34 \cdot 10^{-3}$
590		25,26	1291	6,102	3,525	27,6	$0,47 \cdot 10^{-3}$
600		25,26	1443	6,014	3,525	27,0	$0,30 \cdot 10^{-3}$

where: 2θ - diffraction angle for the most intense peak; I - intensity of the most intense peak; d - interplanar spacing; D - crystallite size; ϵ_{st} - lattice strain.

From Table 3, we observe that a 10 °C change in substrate temperature (T_{sub}) results in a slight variation in the crystallite size, ranging between 32 nm and 27 nm. Simultaneously, the variation in T_{sub} by the same 10 °C step also affects the lattice strain (ϵ_{st}). Similarly, changing the source temperature (T_S) leads to a slight increase in the d parameter, as shown in the T_S variation. This change is more noticeable, ranging from 3.5226 Å (for $T_S=560$ °C) to 3.5250 Å (for $T_S=600$ °C). Additionally, a slight change in the values of crystallite size (D) and lattice strain (ϵ_{st}) is observed with T_S variation, as per Table 3. The minimum value of ϵ_{st} and the largest crystallite size (D) were obtained for samples with $T_{sub}=360$ °C and $T_S=590$ °C. This relationship between T_{sub} and T_S can be attributed to the movement of interstitial Zn atoms within the crystallites at their boundaries, which leads to their dissipation and reduces the concentration of lattice imperfections.

Using the measured reflectance (R) and transmittance (T) spectra along with the thicknesses of ZnTe:O thin films from SEM cross-sections, the absorption coefficient (α) was estimated. The dependence $(\alpha h\nu)^2=f(h\nu)$ for the ZnTe:O thin films deposited at various T_{sub} and T_S is shown in Fig. 5. The estimation of the bandgap energy (E_g) using the Tauc method [7] indicates that E_g decreases from 2.24 eV to 2.19 eV as T_{sub} increases from 320 °C to 360 °C. Regarding the variation in T_S from 560 °C to 600 °C, a different absorption coefficient pattern can be observed at room temperature. From Fig. 5.b, a decrease in the absorption coefficient can be observed with increasing T_S , both in the fundamental absorption regions and in the impurity regions. This phenomenon is caused by the increased thickness of the ZnTe:O thin film with increasing T_S . The estimation of E_g shows a variation of E_g by 0.05 eV, indicating the incorporation of oxygen into the crystalline lattice of ZnTe at $T_{sub}=340$ °C and $T_S=580$ °C.

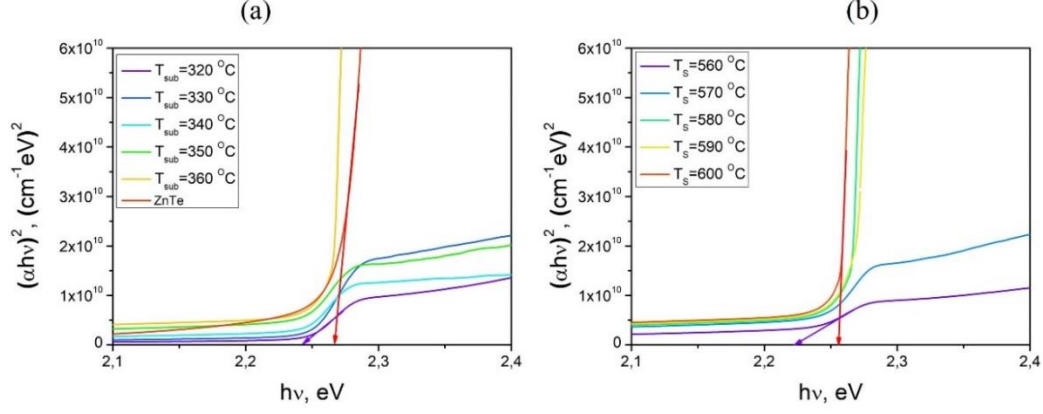


Fig. 5. Dependence of $(ahv)^2=f(hv)$ for ZnTe:O thin films deposited at various T_{sub} (a) and T_s (b).

The photoluminescence (FL) spectra of ZnTe:O thin films deposited at various T_{sub} and T_s are shown in Fig. 6. In all FL spectra, a broad emission band dominates with a maximum at 1.82 eV.

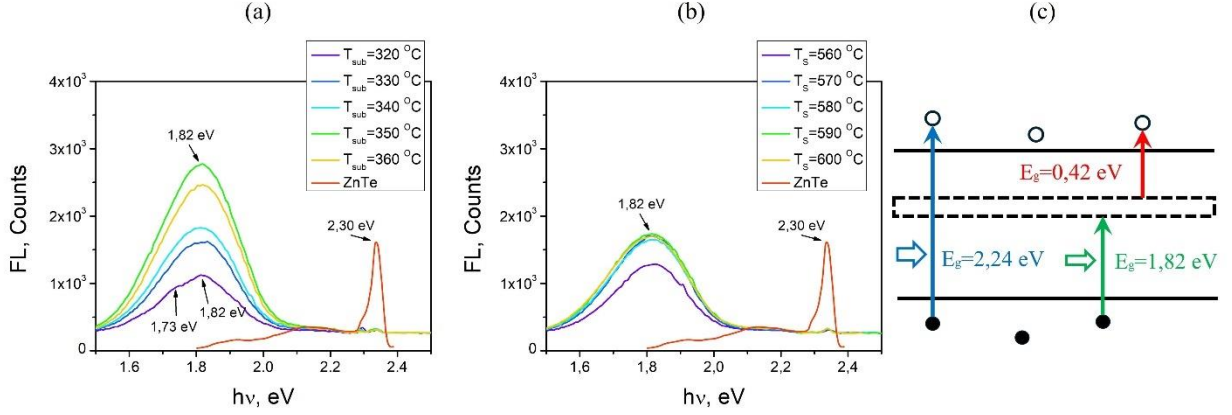


Fig. 6. Photoluminescence spectra of ZnTe:O thin films deposited at various T_{sub} (a) and T_s (b), recorded at $T=300$ K, $\lambda_{ex}=532$ nm, and the energy diagram of ZnTe:O thin films with an intermediate band maximum at 1.82 eV from the valence band (c).

Deconvolution of the FL spectrum of the sample obtained at $T_{sub}=320$ °C using Gauss functions reveals that the emission band consists of two sub-bands (located at 1.82 eV and 1.73 eV), which can be attributed to oxygen centers [8]. Additionally, in all measured spectra, a peak at 2.16 eV is observed. According to study [9], this emission around 2.16 eV is attributed to defects created at grain boundaries or in regions with high dislocation density. This emission is due to native defects (V_{Zn} and Te_i) in the material. Therefore, based on the absorption and FL spectra measured for the first set of samples, it can be assumed that this broad band is associated with the concentration of oxygen ions (O^{2-}), as the band intensity changes with increasing substrate temperature [9]. Figure 6.c illustrates the energy diagram of ZnTe:O thin films.

Therefore, the isoelectronic oxygen impurity creates localized levels like acceptor states near the bottom of the conduction band. These levels resonantly interact with the conduction band, lifting degeneracy and forming new hybrid states, which manifest as two sub-bands with minima

at $k=0$. As a result, the conduction band splits into an upper narrow subband E_+ composed of localized states and a lower broader subband E_- composed of delocalized (extended) states.

Substitutional impurities of O_{Te} in ZnTe provide a pathway for sub-band optical absorption, which is efficient for developing a new generation of intermediate band solar cells (IBSC). These devices are designed to absorb photons with energies lower than the bandgap through an electronic sub-band localized within the bandgap of the host semiconductor. This design enhances the photocurrent production while maintaining the open circuit voltage determined by the bandgap of the host photovoltaic material.

Chapter 4 presents detailed studies on the electrical characteristics of CdS/ZnTe:O structures, employing various methods and measurements to determine essential parameters that influence the efficiency of the heterostructure.

In Figure 7.a, J-V curves are presented under forward bias in a semi-logarithmic scale over the temperature range of 220-350 K. The J-V characteristics exhibit a complex nature, suggesting the involvement of various current transport mechanisms. The current density extrapolated from the direct region of the $\ln J=f(V)$ dependence at $V=0$ yields the value of J_0 , as shown in Table 4, along with electrical parameters. The dependence $\ln(J_0/T^2)=f(1/T)$ for the temperature interval (280-220) K (Figure 7.b) forms a straight line. From the slope of $\ln(J_0/T^2)$ versus $1/T$ and the y-intercept of the respective linear fit, the activation energy (E_A) and the effective Richardson constant (A^{**}) were determined to be 0.98 eV and $69 \text{ A/cm}^2\text{K}^2$, respectively. The barrier height in the temperature range (220-280) K varies from 0.69 eV (at $T=220$ K) to 1.01 eV (at $T=290$ K), while the ideality factor (n_2) varies from 20.78 to 10.95. According to Table 4, the values of the ideality factor n_1 range from 1.96 (at $T=290$ K) to 2.01 (at $T=350$ K). These characteristics allow us to assume that, under forward bias at higher temperatures, the current transport mechanism is dominated by interface recombination. Typically, bulk impurities, surface imperfections, and dislocations serve as recombination paths.

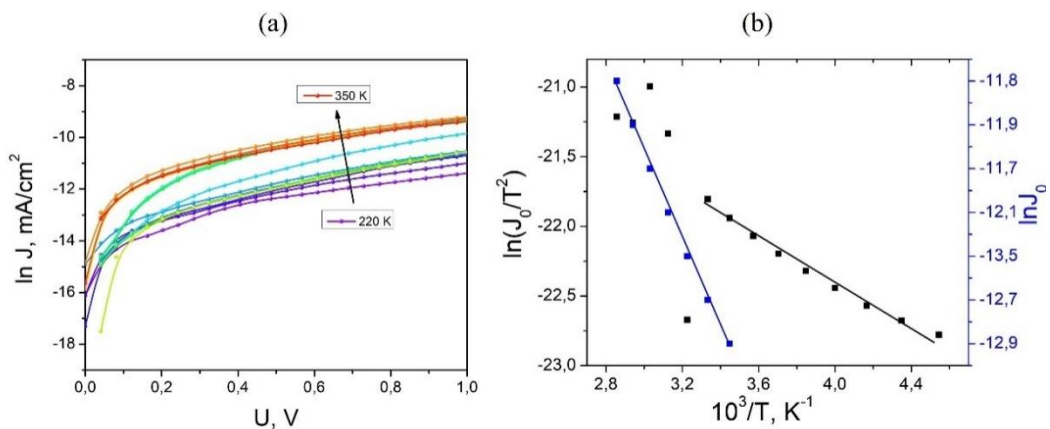


Fig. 7. Dependence $\ln J=f(V)$ (a) and dependence $\ln(J_0/T^2)=f(1/T)$ (b) for the HJ CdS/ZnTe.

Table 4. Electrical parameters of the CdS/ZnTe HJ at various measurement temperatures.

T, K	$\ln J_0$	$J_0, 10^{-2}$ mA/cm^2	n_1 ($U < 0,2 V$)	n_2 ($U > 0,2 V$)	$q\Phi_{b0}, eV$	V_d, V
220	-13,0	0,62	1,76	20,78	0,69	0,43
230	-12,8	0,75	1,34	15,63	1,1	0,69
240	-12,6	0,91	0,83	13,33	1,26	0,79
250	-12,4	1,12	1,71	13,82	1,34	0,84
260	-12,2	1,37	2,41	13,18	1,17	0,73
270	-12,0	1,67	2,56	11,98	1,31	0,82
280	-11,8	2,04	2,08	11,88	1,39	0,68
290	-11,6	2,49	1,96	10,95	1,01	0,63
300	-11,4	3,05	2,18	10,67	1,39	0,87
310	-12,2	1,37	1,97	12,05	1,61	1,01
320	-10,8	5,56	1,96	11,09	1,15	0,72
330	-10,4	8,30	1,81	12,49	1,15	0,72
340	-10,6	6,79	1,60	11,33	1,33	0,83
350	-10,5	7,50	2,01	12,10	1,61	1,01

The study of the C-V dependence of the CdS/ZnTe HJ at different frequencies (10 kHz, 100 kHz, 1 MHz) indicates cyclic variation or hysteresis in the C-V curve shape. As the measurement frequency increases from 10 kHz to 1 MHz, the capacitance value of the CdS/ZnTe structure decreases by nearly an order of magnitude, suggesting the contribution of states at the heterostructure interface. Figure 8 shows the capacitance dependence with two slopes: one for negative voltages and another for positive voltages, indicating two different mechanisms contributing to capacitance in these voltage regions. These mechanisms arise from distinct responses of fixed and mobile charges between the interface region and the volume of the HJ. The interface state density at CdS/ZnTe reaches $4.9 \cdot 10^{10} \text{ eV}^{-1} \text{ cm}^{-2}$. C-V measurements also allow us to estimate the thickness of the space charge region, which varies with measurement frequency from $2.16 \mu\text{m}$ (at 10 kHz) to $4.33 \mu\text{m}$ (at 1 MHz). In the whole temperature ranges, there is a slight variation around the threshold voltage value of 1.2 V (V_d). The density of acceptor states (denoted as N_A), estimated from the linear slope of the $C^{-2}=f(V)$ dependencies, reaches values of $0.81 \cdot 10^{17} \text{ cm}^{-3}$ (at 350 K), $1.22 \cdot 10^{17} \text{ cm}^{-3}$ (at 300 K), and $3.23 \cdot 10^{14} \text{ cm}^{-3}$ (at 220 K).

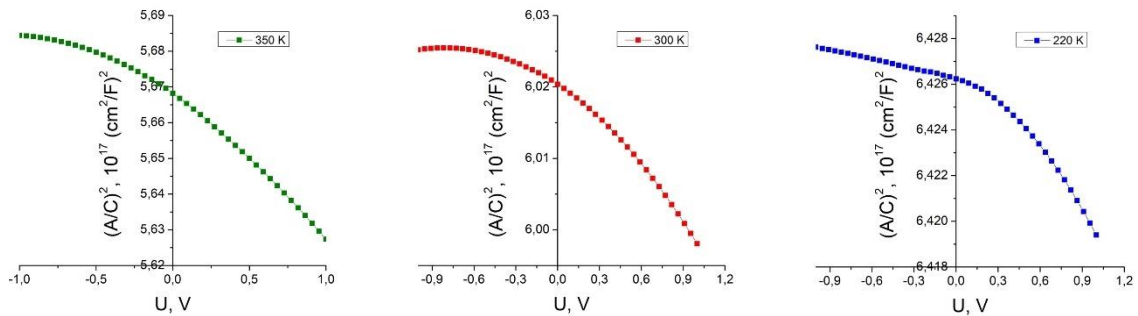


Fig. 8. The dependence of $(1/C)^2=f(V)$ for the CdS/ZnTe HJ at various measurement temperatures

To construct the energy band diagram of a heterojunction, it is essential to use data from the current-voltage characteristics (J-V) and capacitance-voltage characteristics (C-V), along with knowledge of the electron affinities and Fermi level positions for each component material. The numerical data have been presented in Table 5.

Table 5. Electrical parameters of the CdS/ZnTe HJ obtained from experimental data

Parameters	CdS	ZnTe
E_g , eV	2,40	2,20
χ , eV	4,5	3,5
Effective mass, m^*	0,17 m_0	0,12 m_0
m_0 , kg	$9,1 \cdot 10^{-31}$	
Lattice parameter a și c , Å	$a=4,141$ $c=6,720$	$a=6,103$
N_D , cm^{-3}	$9,0 \cdot 10^{19}$	-
N_A , cm^{-3}	-	$3,55 \cdot 10^{15}$
N_V , cm^{-3}	-	$2,24 \cdot 10^{18}$
N_C , cm^{-3}	$2,41 \cdot 10^{18}$	-
ϵ_r	9,35	10,3
HJ		
E_C-E_F , eV	-0,07	
E_F-E_V , eV	0,17	
ΔE_C , eV	0,9	
ΔE_V , eV	-0,72	

Based on the data from Table 5, the energy band diagrams of the CdS/ZnTe HJ were constructed for voltages below 0.2 V (Fig. 9.a) and above 0.2 V (Fig. 9.b).

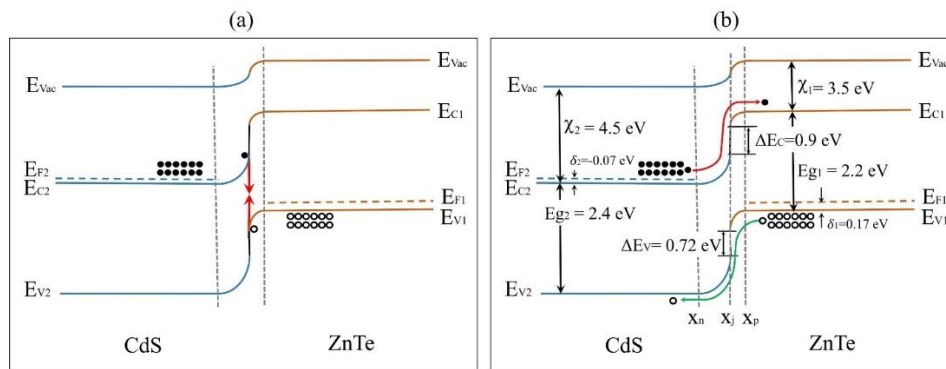


Fig. 9. Energy band diagrams of HJ CdS/ZnTe at forward bias below 0.2 V (a) and above 0.2 V (b).

Additionally, measurements of capacitance (C) and G/ω (real part of normalized conductance as a function of frequency) were conducted at various frequencies and temperatures.

Fig. 10 depicts how capacitance varies with frequency for various measurement temperatures. The graph highlights a plateau between 1 MHz and 100 kHz, indicating that capacitance remains relatively constant within this frequency range. Subsequently, there is a period

of dielectric relaxation at frequencies above 10^5 Hz. Fig. 10.b illustrates how the dielectric constant depends on temperature for different measurement frequencies in the case of HJ CdS/ZnTe. It can be observed that the dielectric constant behaves similarly to capacitance, increasing gradually and monotonically with temperature.

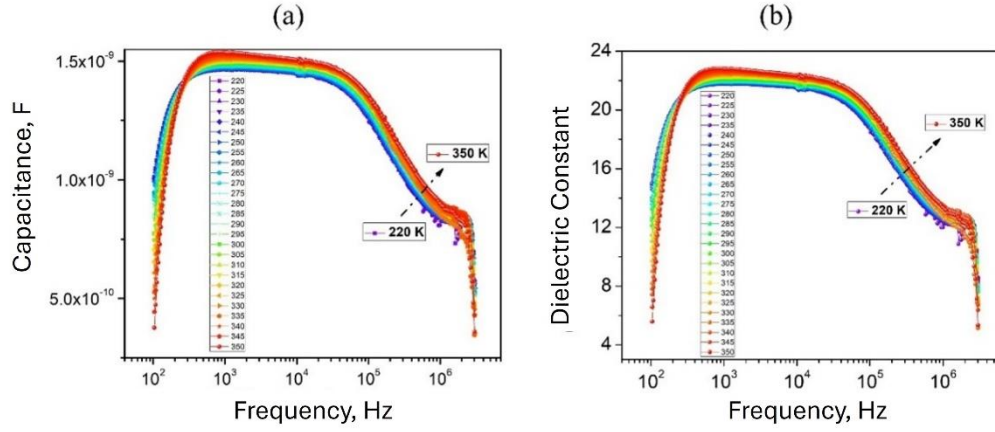


Fig. 10. Variation of capacitance (a) and dielectric constant (b) with frequency of HJ CdS/ZnTe for different measurement temperatures

The loss angle tangent ($\tan\delta$) or dissipation factor can be directly extracted from measurement data. It is known that the electric induction vector represents the tangent of the loss angle, i.e., $\tan\delta = \vec{D}$. Fig. 11.a illustrates the dependence of $\tan\delta = f(T)$ for various measurement frequencies. It can be observed that with increasing frequency at all studied temperatures, $\tan\delta$ decreases, likely due to a reduction in the alignment degree of electric dipoles in molecules. However, starting from around 10 MHz, $\tan\delta$ begins to increase again. Fig. 11.b illustrates how the total conductivity σ varies with frequency. At low frequencies, there is behavior independent of frequency, corresponding to direct current conductivity, whereas at high frequencies, the alternating component of conductivity predominates. The alternating conductivity is influenced not only by temperature but also by frequency:

$$\sigma_{ac} = A\omega^S, \quad (1)$$

where A represents a constant, ω is the angular frequency, and S is an exponent typically with a value less than or equal to one.

The value and behavior of the exponent S in equation (1) with respect to temperature and/or frequency determine the predominant conduction mechanism in the material. Depending on the value and behavior of S , several theoretical models have been developed to explain the conduction mechanism of materials (QMT, SPT, LPT, and CBH).

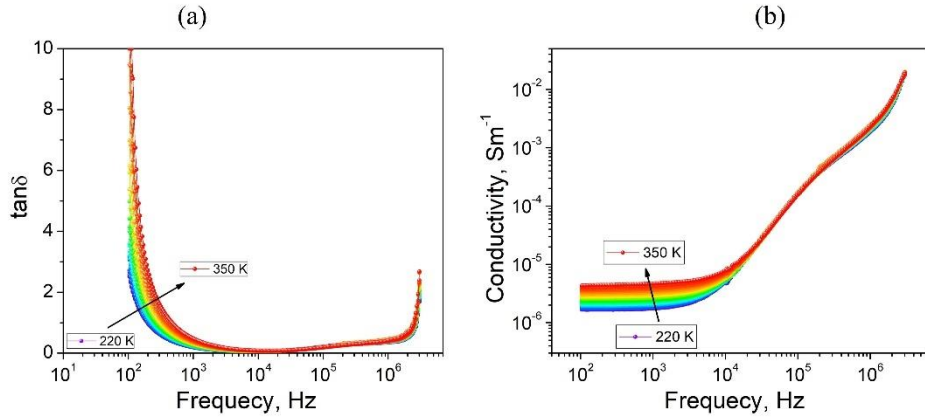


Fig. 11. Dependence of $\tan\delta=f(\text{frequency})$ (a) and total conductivity (b) of HJ CdS/ZnTe for various measurement temperatures.

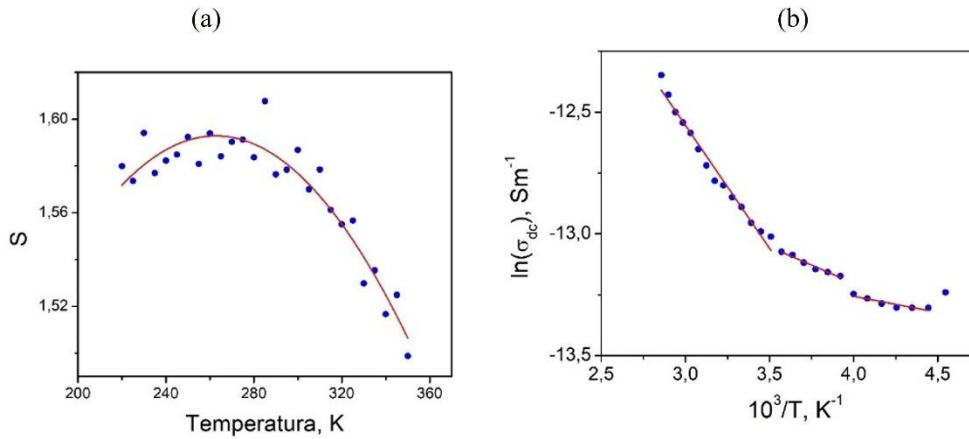


Fig. 12. Exponent S (a) and DC conductivity σ_{DC} (b) as a function of measurement temperature for HJ CdS/ZnTe.

Within the Quantum Mechanical Tunneling (QMT) model, it is suggested that S is influenced by frequency but not by temperature. In the tunneling model (SPT), it is predicted that S increases as temperature rises. For the tunneling (LPT) model, S depends on both temperature and frequency. In the Correlated Barrier Hopping (CBH) model, where conduction arises from synchronized hopping of charge carriers between nearest neighboring states, it is assumed that S depends on both temperature and frequency, and S should decrease as temperature increases (Fig. 12.).

In the dependence of conductivity on frequency, two distinct regions can be observed near the frequency of 100 kHz, where a dielectric relaxation in conductivity is noted. At higher frequencies, conductivity decreases significantly as frequency increases, suggesting a tendency towards direct current electrical conductivity around 100 kHz. At this point, a new dielectric relaxation is observed leading to a pronounced drop in conductivity, which remains steady until frequencies of 10^5 Hz. Through analysis of these two regions depicted in the graph measured at

350 K, according to Jonscher's law, it has been determined that the variation of conductivity with frequency follows the parameter S value of 1.63 at low frequencies (1 MHz - 5 MHz) and 2.7 at frequencies greater than 5 MHz. As observed in Fig. 12.b, the relationship between conductivity and temperature exhibits a linear variation over the temperature range of 280-350 K. This suggests that the behavior of the CdS/ZnTe structure resembles that of a ferroelectric crystal with ionic conductivity described by the equation:

$$\sigma_{dc} = \sigma_0 \exp\left(-\frac{E_a}{k_B T}\right). \quad (2)$$

In the temperature range of 280-350 K, where the activation energies are $E_{a1}=0.98$ eV, $E_{a2}=0.90$ eV, and $E_{a3}=0.86$ eV, the conductivity of the CdS/ZnTe structure follows an exponential relationship with temperature.

To confirm the conductivity component's behavior in the temperature range of 220-280 K, the electrical impedance of HJ CdS/ZnTe was analyzed. Fig. 13.a presents the frequency dependence of the real component Z' and imaginary component Z'' of the complex impedance $Z=Z'-iZ''$ (where $i= -1$) for HJ CdS/ZnTe with a silver contact area of 0.3 cm², in the frequency range of 100 Hz to 10 MHz at various temperatures. Complex impedance measurements of the sample provide useful information about the real part Z' (resistive part) and the imaginary part Z'' (reactive part) of the complex impedance. It is known that for a sample with introduced capacitance in an alternating electromagnetic field of frequency ω , the equivalent electrical circuit of HJ CdS/ZnTe:O [10] is depicted in Fig. 13.b.

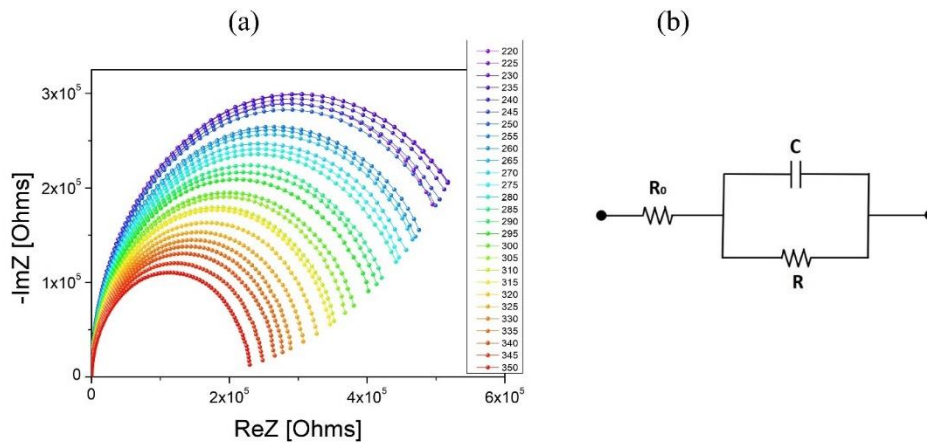


Fig. 13. Graphical dependence of impedance spectra of HJ CdS/ZnTe (a) and the equivalent circuit of a sample used in complex impedance measurement (b).

Complex electrical conductivity σ of the sample consists of the components σ' and σ'' , representing the real and imaginary parts of the complex electrical conductivity, respectively. These can be expressed by the relationships:

$$\sigma' = \frac{\rho'}{M'} \quad (3)$$

and

$$\sigma'' = \frac{\rho''}{M'} \quad (4)$$

where M represents the complex modulus of impedance, defined by the relation:

$$M = |Z^*|^2 \cdot \left(\frac{A}{d}\right)^2, \quad (5)$$

where $Z^* = \sqrt{Z'^2 + Z''^2}$ represents the complex modulus of impedance of HJ CdS/ZnTe. The complex modulus of impedance (M'') of HJ CdS/ZnTe is shown in Fig. 14.a. M'' exhibits a maximum that shifts to higher frequencies with increasing temperature, indicating a correlation with the movements of mobile ionic charges. The frequency region where peaks appear indicates the transition of charge carriers from long-range to short-range mobility. Such results may be caused by a lack of restoring force governing the mobility of charge carriers under induced electric field. This behavior suggests that as frequency increases, each ion travels on a progressively shorter path until the electric field changes so rapidly that ions only move within the energy potential well boundaries, performing localized motion within it. We observe that the maximum of interfacial polarization shifts to higher frequencies as the measurement temperature increases, indicating the existence of two dielectric relaxation processes described by the Vogel-Fulcher-Tammann (VFT) law.

According to Debye's theory [11], the relationship between the peak frequency ω_{max} where the imaginary component Z'' reaches its maximum, and the relaxation time constant (τ), which represents the time after which the oscillation amplitude decreases to 1/e of its maximum value, is described by the equation:

$$2\pi\omega_{max}\tau = 1. \quad (6)$$

Using the experimental values of the peak frequency ω_{max} the relaxation time constant τ was estimated, and the dependence $\ln\tau=f(1/T)$ was plotted, as shown in Fig. 14.b.

A nonlinear dependence can be observed between the natural logarithm of the relaxation time and the versus of temperature. The data on dielectric relaxation time is shown in Fig. 14. adhere to the Vogel-Fulcher-Tammann (VFT) relationship, which is widely used to describe the dynamics of relaxation in various structures:

$$\tau(T) = \tau_{\infty} \left[\frac{-DT_0}{R(T - T_0)} \right], \quad (7)$$

where T_0 is the Vogel temperature, also known as the transition temperature, τ_{∞} is the time at which the temperature T tends towards infinity ($T \rightarrow +\infty$), R is the universal gas constant, and D is the

specific constant of the VFT relationship. The very low values of Vogel temperature indicate that the relaxation time for all samples conforms to classical law.

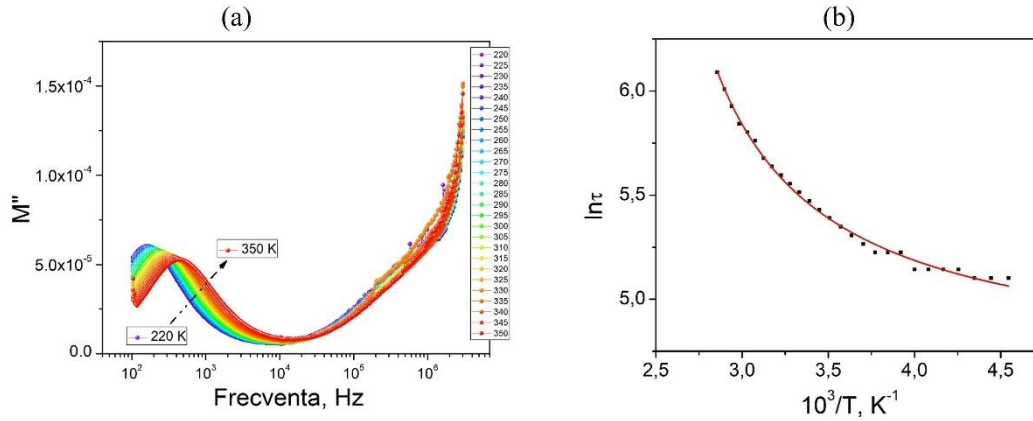


Fig. 14. Dependency of the complex impedance modulus (M'') (a) and the dependence $\ln\tau=f(1/T)$ (b) of HJ CdS/ZnTe

Therefore, the interaction between ionic conductivity and interfacial polarization is a key point for understanding the current transport mechanism in HJ nCdS/pZnTe.

In **Chapter 5**, the parameters in photovoltaic mode are presented: open-circuit voltage (V_{OC}), short-circuit current density (J_{SC}), fill factor (FF), external quantum efficiency (EQE), and conversion efficiency (η) as a function of technological conditions. The integral photoelectric characteristics show the dependence of short-circuit current density and open-circuit voltage on illumination.

Fig. 15.a shows the J-U characteristics of HJ CdS/ZnTe obtained at different substrate temperatures (T_{sub}). The best open-circuit voltage (V_{OC}), which was 0.48 V, was recorded at a substrate temperature of 340 °C, while the best short-circuits current density value (J_{SC}), of 1.15 A/cm², was observed in the structure deposited at 360 °C. In the second set, we varied the source temperature (T_S) between 560 °C and 600 °C, while keeping the substrate temperature constant at 340 °C. The best short-circuit current density was recorded for $T_S=580$ °C, while the best open-circuit voltage was obtained for $T_S=600$ °C.

The design and technologies used for the back contact can vary depending on the type of photovoltaic device and the materials used. The main goal of this contact is to maximize the generation of electrical energy from the visible spectrum absorbed by the cell. In this context, a set of CdS/ZnTe photovoltaic cells was fabricated using various metals for the back contact of ZnTe. The J-V characteristics of these cells, measured under illumination of 100 mW/cm², with different metals at the back contact, are presented in Fig. 16.a. The back contact significantly influences the efficiency of photovoltaic cells because ZnTe has a high work function value of 5.3-

5.8 eV. The contact resistance between ZnTe and the metals Cu, Pd/Ag, Ni, Ag was calculated based on the J-V characteristics of Cu/ZnTe, Ni/ZnTe, Ag/ZnTe, and Pd/Ag/ZnTe structures. It was observed that the most suitable metal for the CdS/ZnTe structure is Ag, deposited via a paste.

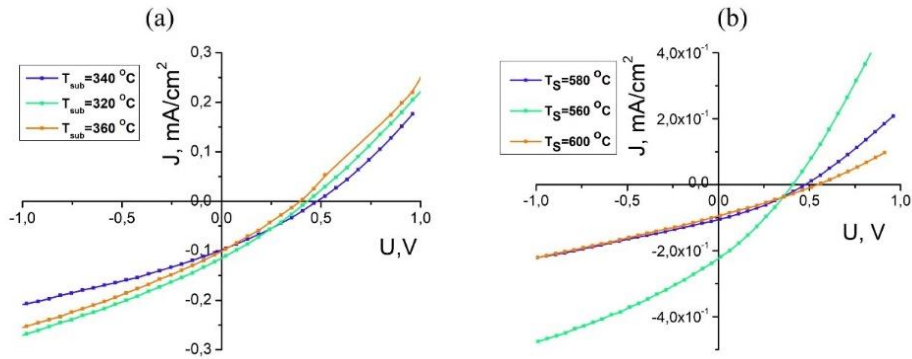


Fig. 15. J-V characteristics of HJ CdS/ZnTe obtained at different substrate temperatures (a) and source temperatures (b) under illumination of 100 mW/cm², 300 K

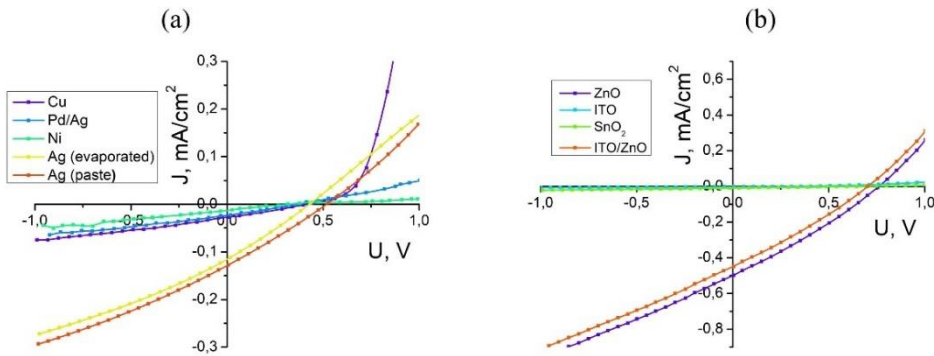


Fig. 16. J-V characteristics of HJ CdS/ZnTe with different metals for the back contact (a) and with different front contacts (b), under illumination of 100 mW/cm², 300 K

The front contact of a photovoltaic cell, which directly contacts sunlight, plays a crucial role in collecting and directing the generated electric current. It is located opposite the back contact on the surface of the structure. The front contact can be made up of multiple thin and functional layers, such as layers of conductive materials and anti-reflective coatings. To optimize performance, a set of samples with different transparent conductive oxides (TCO) was obtained. From Fig. 16.b, the most efficient TCO is ZnO, presenting maximum efficiency.

Thus, in the research of photoelectric properties, two types of photovoltaic cells with better photovoltaic parameters were established: CdS/ZnTe:O/PEDOT:PSS/Ag and CdS/ZnTe:Mn/Ag, whose technology can be reproduced. The following technological steps were followed in the fabrication process: ZnO was used as the front contact; a thin films of CdS (~200 nm) was deposited over the ZnO thin films; the ZnTe:O absorber layer was deposited at $T_{sub}=340$ °C and $T_s=600$ °C, with a deposition time of 18 minutes; after the deposition of the ZnTe absorber layer, a thin films of PEDOT:PSS was applied by spin-coating, functioning as a buffer layer at the back

contact; a silver conductive paste was used to create the back contact. As a result of these steps, the following characteristics were obtained for the CdS/ZnTe/PEDOT:PSS/Ag photovoltaic cell: open-circuit voltage $V_{OC}=0.84$ V, short-circuit current $J_{SC}=0.25$ mA/cm², fill factor $FF=38.6\%$, and a solar-to-electric energy conversion efficiency of 0.1% (Fig. 17).

Table 6. Photovoltaic parameters of the best HJ CdS/ZnTe

Samples	V_{OC} , V	J_{SC} , mA/cm ²	FF , %	η , %
CdS/ZnTe:O	0,84	0,25	38,6	0,1
CdS/ZnTe:Mn	0,47	0,24	34,2	0,05

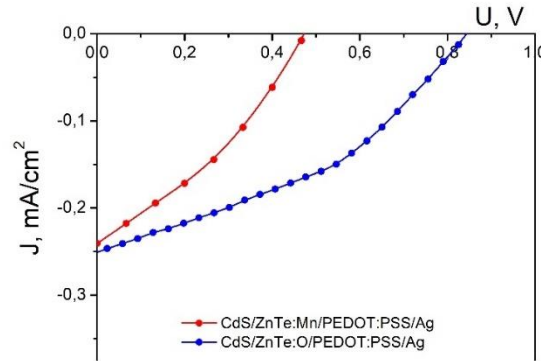


Fig. 17. J-V characteristics of the best HJ CdS/ZnTe

In the obtained photovoltaic cells, only a portion of the incident radiation energy is converted. Most of the energy is lost due to various phenomena during conversion. These phenomena include reflection of light from the semiconductor surface; transmission of light through the semiconductor without absorption; dissipation of energy of electrons and holes generated by photons with $h\nu > E_g$; reduction in the concentration of non-equilibrium charge carriers due to their recombination at the semiconductor surface and within its volume; losses due to resistances R_S and R_{sh} . The external quantum efficiency (Fig. 18.) of the HJ CdS/ZnTe with evaporated Ag as ohmic contact is nearly 0.2 at the peak located at the wavelength of 550 nm, while the internal quantum efficiency is higher than the external quantum efficiency.

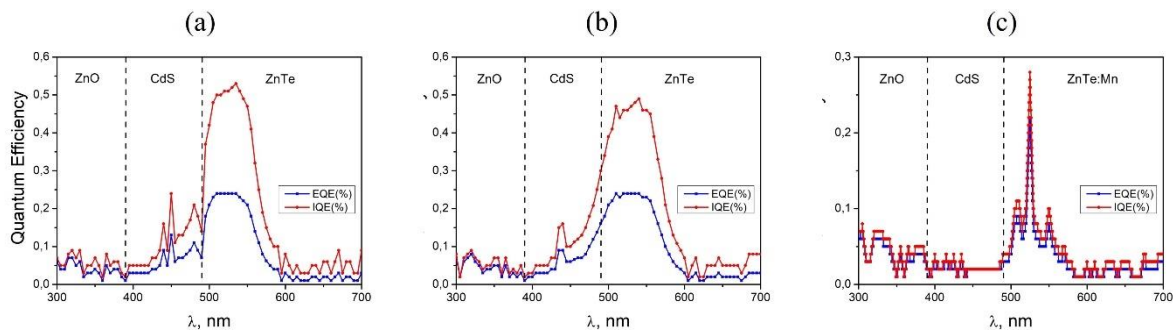


Fig. 18. Spectral distribution of internal and external quantum efficiency of HJ CdS/ZnTe/PEDOT:PSS/Ag (from paste) (a), CdS/ZnTe/PEDOT:PSS/Ag evaporated (b), and CdS/ZnTe:Mn/PEDOT:PSS/Ag from paste (c)

The buffer layer deposited on the ZnTe absorber before the Ag contact deposition by evaporation increases the internal quantum efficiency to nearly 0.5, while the external quantum efficiency remains unchanged at 0.2. The internal quantum efficiency of HJ CdS/ZnTe with PEDOT:PSS buffer layer and ohmic contact deposited from Ag paste indicates a slightly higher value of internal quantum efficiency, just above 0.5, while the external quantum efficiency remains at 0.2.

In the case of doping the ZnTe thin films with Mn, both the internal and external quantum efficiency values decrease to 0.1. In all photovoltaic cell designs, the internal and external quantum efficiency at longer wavelengths is limited by E_g of ZnTe.

GENERAL CONCLUSIONS

1. The J-V characteristics of the CdS/ZnTe photovoltaic device were simulated using the following input parameters: $d_{\text{ZnTe}}=1,0 \mu\text{m}$, $d_{\text{CdS}}=5 \text{ nm}$, $d_{\text{ZnO}}=20 \text{ nm}$, $E_{g(\text{ZnTe})}=2,2 \text{ eV}$, $E_{g(\text{CdS})}=2,4 \text{ eV}$, $E_{g(\text{ZnO})}=3,3 \text{ eV}$, $\Phi_{(\text{Ag})}=4,7 \text{ eV}$ with the SCAPS-1D software, and the following photovoltaic parameters: $V_{OC}=0,89 \text{ V}$, $J_{SC}=25,9 \text{ mA/cm}^2$, $FF=72,6$, $\eta=16,78\%$.
2. Optimal technological conditions were developed for obtaining thin films of ZnTe, CdS using the close space sublimation method, and ZnO thin films using the spray pyrolysis method. The CdS thin films exhibited a hexagonal polycrystalline structure regardless of the treatment environment. Vacuum treatment at $T=400 \text{ }^\circ\text{C}$ for one hour allows obtaining polycrystalline layers with crystallite size of 0.48 nm , average transmittance of approximately 85% , and bandgap values (E_g) around $2.40 \text{ eV} \pm 0.02 \text{ eV}$, regardless of the annealing environment. Studies on ZnTe:O thin films obtained at substrate temperature (T_{sub}) ranging from $320 \text{ }^\circ\text{C}$ to $360 \text{ }^\circ\text{C}$ and source temperature (T_S) ranging from $560 \text{ }^\circ\text{C}$ to $600 \text{ }^\circ\text{C}$ indicated the optimal conditions as $T_{sub}=340 \text{ }^\circ\text{C}$ and $T_S=600 \text{ }^\circ\text{C}$. The obtained ZnTe thin layers exhibited a zincblende structure, classified under space group F43m (216) with preferred orientation [1 1 1].
3. After deposition, the ZnTe thin films obtained at different T_{sub} and T_S were annealed in O_2 flux at $400 \text{ }^\circ\text{C}$ for 60 minutes. EDX analysis indicated that oxygen was incorporated into the crystalline lattice of ZnTe, with its concentration decreasing from 5.88% (for $T_S=560 \text{ }^\circ\text{C}$) to 0.6% (for $T_S=600 \text{ }^\circ\text{C}$), while increasing with T_{sub} , reaching 4.49% at $T_{sub}=360 \text{ }^\circ\text{C}$. These results suggest the formation of a diluted semiconductor alloy with an intermediate band in the oxygen-doped ZnTe thin films.
4. Transmission and reflectance spectra analysis revealed that increasing substrate temperature (T_{sub}) from $320 \text{ }^\circ\text{C}$ to $360 \text{ }^\circ\text{C}$ altered the E_g value of the ZnTe:O thin films from 2.24 eV to 2.19 eV , while source temperature (T_S) did not affect the E_g value. Photoluminescence (PL) spectra of the layers obtained in the $T_{sub}=320 - 360 \text{ }^\circ\text{C}$ range were dominated by broad bands located at 1.73 eV and 1.82 eV , whose positions were determined by the substrate temperature, whereas only the 1.82 eV band predominated with T_S variation, attributed to the intermediate band formed by the oxygen isoelectronic impurity.
5. Undoped and Al-doped ZnO thin films, regardless of the atmosphere during formation, exhibited a hexagonal polycrystalline structure with preferred orientation [0 0 2]. The highest crystallinity was observed in the structure doped with 1% Al in an O_2 atmosphere,

where $D=31$ nm, $\varepsilon_{st}=1.4 \cdot 10^{-3}$. Topographic study indicated that surfaces of ZnO thin films obtained in an O₂ atmosphere were rougher, with $R_{MS}=60.96$ nm and $R_a=1.45$ nm, yet showing average transmittance of ~90%, $E_g=3.22$ eV, conductivity of 1316 ($\Omega \cdot \text{cm}$)⁻¹, and charge carrier concentration of $1,25 \cdot 10^{21}$ cm⁻³.

6. The technology for fabricating CdS/ZnTe:O structures involved using ZnO (~400 nm) as the front contact, followed by a thin CdS thin films (~200 nm) annealed in vacuum. Subsequently, the ZnTe:O absorber layer (~3.0 μm) was grown via CSS method, followed by application of a PEDOT:PSS thin films via spin-coating, serving as a buffer layer at the back contact. Silver paste was used to create back contact.
7. According to the C-V characteristics of the CdS/ZnTe:O structures, the thickness of the space charge region varied with the capacitance measurement frequency, ranging from 2.16 μm at 10 kHz to 4.33 μm at 1 MHz, located within ZnTe, while the density of states at the interface between CdS and ZnTe reached a value of $4.9 \cdot 10^{10}$ eV⁻¹cm⁻². The effective concentration of acceptor impurities at room temperature reached $7.4 \cdot 10^{14}$ cm⁻³.
8. The J-V and C-V characteristics of the CdS/ZnTe:O structures indicated that the forward current was dominated by thermionic emission and recombination through interface states and traps at all temperatures, with higher temperatures exceeding room temperature exhibiting more intense recombination through interface states and traps than the thermionic emission component. The total conductivity at low frequencies corresponded to ionic conductivity, while at higher frequencies, it exhibited interface polarization conductivity.
9. The study of the J-V characteristics under full sunlight illumination of 100 mW/cm² showed that increasing the thickness of the ZnTe:O absorber layer in the CdS/ZnTe:O photovoltaic cell resulted in an increase in open-circuit voltage and short-circuit current density to their maximum values of $V_{OC}=0.84$ V and $J_{SC}=0.25$ mA/cm². The energy conversion efficiency reached 0.13%. Internal quantum efficiency indicated a value higher than 0.5 in the wavelength range of 490-590 nm.

RECOMMENDATION

Simulation of the J-V characteristics of the CdS/ZnTe heterojunction indicates a solar-to-electric conversion efficiency of 16.78%. To experimentally achieve this value, it is necessary to optimize the technology for obtaining ZnTe thin films. Analysis of the structural and optical properties of the ZnTe thin films confirms the formation of a diluted semiconductor alloy due to annealing in oxygen at 420 °C for 40 minutes, resulting in the formation of an O_{Te} intermediate band. Unfortunately, during annealing, this band disappears due to diffusion of the component elements of the "window layer" and absorber, forming a layer at the interface with a bandgap smaller than that of ZnTe, capturing almost all free charge carriers on network imperfections at the HJ interface. To successfully achieve a diluted ZnTe semiconductor alloy in the junction structure, it is necessary to:

- a) increase the distance between the source and substrate in the ZnTe evaporation system and oxygen doping during deposition in the vacuum chamber to achieve a higher oxygen concentration;
- b) develop a technological process for obtaining components that eliminates diffusion of the structure's component elements;
- c) propose a different buffer layer than CdS;
- d) Use metals or alloys as ohmic contacts whose electron extraction work function is greater than 5.5 eV.

BIBLIOGRAPHY

1. YANG, Y., HOANG, M., BHARDWAJ, A., WILHELM, M., MATHUR, S., WANG, H. Perovskite solar cells based self-charging power packs: Fundamentals, applications and challenges. In: *Nano Energy*. 2022, nr. 94, pp. 106910.
2. TURKAY, D., ARTUK, K., CHIN, X., JACOBS, D., MOON, S., WALTER, A., WOLFF, C. High-efficiency (> 30%) monolithic perovskite-Si tandem solar cells with flat front-side wafers. In: *Research Square*. 2023.
3. KAPADNIS, R., BANSODE, S., SUPEKAR, A., BHUJBAL, P., KALE, S., JADKAR, S., PATHAN, H. (2020). Cadmium telluride/cadmium sulfide thin films solar cells: a review. In: *ES Energy & Environment*. 2020, nr. 10(20), pp. 3-12.
4. SCARPULLA, M., MCCANDLESS, B., PHILLIPS, A., YAN, Y., HEBEN, M., WOLDEN, C., HAYES, S. CdTe-based thin film photovoltaics: Recent advances, current challenges and future prospects. In: *Solar Energy Materials and Solar Cells*. 2023, nr. 255, pp. 112289.
5. WANG, W., LIN, A., PHILLIPS, J. Intermediate-band photovoltaic solar cell based on ZnTe: O. In: *Applied Physics Letters*. 2009, nr. 95(1).
6. SINGH, H., SINGH, T., SHARMA, J. Review on optical, structural and electrical properties of ZnTe thin films: effect of deposition techniques, annealing and doping. In: *ISSS Journal of Micro and Smart Systems*. 2018, nr. 7(2), pp. 123-143. Disponibil: DOI: 10.1007/s41683-018-0026-2
7. YANG, Q., LIU, C., CUI, L., ZHANG, L., ZENG, Y. Structural, surface, and electrical properties of nitrogen ion implanted ZnTe epilayers. In: *Applied Physics A*. 2014, nr. 116, pp. 193-197.
8. GARCIA, J., REMON, A., MUNÑZ, V., TRIBOULET, R. Annealing-induced changes in the electronic and structural properties of ZnTe substrates. In: *Journal of Materials Research*. 2000, nr. 15, pp. 1612-1616.
9. NISHIO, M., HAYASHIDA, K., GUO, Q., OGAWA, H. Effect of VI/II ratio upon photoluminescence properties of aluminum-doped ZnTe layers grown by MOVPE. In: *Applied Surface Science*. 2001, nr. 169-170, pp. 223–226. DOI: 10.1016/s0169-4332(00)00655-3
10. SCAIFE, B. Principles of dielectrics. 1989.
11. DEBYE, P. Polar Molecules. Dover, New York, 1929.

LIST OF AUTHOR'S PUBLICATIONS ON THESIS TOPIC

1. Specialized books (recommended for publication by the senate/scientific council of an organization in the fields of research and innovation or recognized as scientific books abroad: review process, approval by scientific organizations, or publication by prestigious scientific publishers)

1.1. Single-author specialized books

1.2. Specialized collective books (with specification of individual contributions)

2. Articles in scientific journals

2.1. in Web of Science and SCOPUS indexed journals

1) **LUNGU, Ion**, ZALAMAI, Victor, MONAICO, Eduard, GHIMPU, Lidia, POTLOG, Tamara. Effect of deposition temperature on structural, morphological and optical properties of ZnTe thin films. In: *Journal of Materials Science*. 2023, nr. 10(58), pp. 4384-4398. ISSN 0022-2461. DOI: <https://doi.org/10.1007/s10853-023-08285-x> (IF:4.5)

2) **LUNGU, I**, PATRU, R, GALCA, A, PINTILIE, L, POTLOG, T. (2024). DC current-voltage and impedance spectroscopy characterization of nCdS/pZnTe HJ. In: *Scientific reports*, 2024, nr.14(1), pp. 12955. (IF:4.6)

3) **LUNGU, Ion**, POTLOG, Tamara. Thermally Annealed in Vacuum Undoped and Al-Doped ZnO Thin Films for Multifunctional Applications. In: *Lecture Notes in Networks and Systems*. 2020, nr. 101, pp. 144-158. ISSN 2367-3370. DOI: https://doi.org/10.1007/978-3-030-36841-8_15

2.2. in journals indexed in other ANACEC-accepted databases (with specification of the database)

2.3. in journals from the National Register of Profile Journals (specifying the category)

Cat. B:

1) **LUNGU, Ion**. Efectul dopării straturilor de ZnTe cu cupru asupra parametrilor fotovoltaici ai heterostructurilor ZnTe:Cu/CdTe. In: *Studia Universitatis Moldaviae. Seria Științe Exacte și Economice*. 2021, nr. 2(142), pp. 73-77. ISSN 1857-2073. DOI: <https://doi.org/10.5281/zenodo.5094790>

2) **LUNGU, Ion**. Influența dopării cu aluminiu asupra proprietăților optice ale straturilor subțiri de ZnO. In: *Studia Universitatis Moldaviae. Seria Științe Exacte și Economice*. 2020, nr. 7(137), pp. 23-30. ISSN 1857-2073. DOI: <https://doi.org/10.5281/zenodo.4457488>

Cat. C:

1) **LUNGU, Ion**, GHIMPU, Lidia, UNTILA, Dumitru, POTLOG, Tamara. Copper-related defects in ZnTe thin films grown by the close space sublimation method. In: *Moldavian Journal of the Physical Sciences*. 2022, nr. 1(21), pp. 34-41. ISSN 1810-648X. DOI: <https://doi.org/10.53081/mjps.2022.21-1.03>

2) **LUNGU, Ion**, GAGARA, Ludmila, GHIMPU, Lidia, POTLOG, Tamara. Synthesis and electrophysical properties of CdS/ZnTe heterojunctions. In: *Moldavian Journal of the Physical Sciences*. 2022, nr. 1(21), pp. 42-51. ISSN 1810-648X. DOI: <https://doi.org/10.53081/mjps.2022.21-1.04>

3) **RUSNAC, Dumitru**, **LUNGU, Ion**, GHIMPU, Lidia, COLIBABA, Gleb, POTLOG, Tamara. Structural and optical properties of ZnO:Ga thin films deposited on ITO/glass substrates for optoelectronic applications. In: *Moldavian Journal of the Physical Sciences*. 2021, nr. 1(20), pp. 84-93. ISSN 1810-648X. DOI: <https://doi.org/10.53081/mjps.2021.20-1.07>

3. Articles in conference proceedings and other scientific events

3.1. in proceedings of scientific events included in Web of Science and SCOPUS databases

- 1) POTLOG, Tamara, GORCEAC, Leonid, TAKU, Miyake, **LUNGU, Ion**, RAEVSCHI, Simion, WORASAWAT, Suchada, BOTNARIUC, Vasile, MIMURA, Hidenori. Synthesis and Properties of Al-doped ZnO Thin Films for Photovoltaics. In: *Proceedings. 4th International Conference on Nano Electronics Research and Education (ICNERE)*, 2018, Hamamatsu, Japan, pp. 1-6, DOI: 10.1109/ICNERE.2018.8642595. <https://ieeexplore.ieee.org/abstract/document/8642595>
- 2) **LUNGU, Ion**. Structural and composition of Cu-doped ZnTe thin films with different concentrations by immersion in Cu(NO₃)₂ solution. In: *Proceedings of the International Semiconductor Conference CAS*. Ediția a 44-a, 6-8 octombrie 2021, Sinaia. New Jersey, USA: Institute of Electrical and Electronics Engineers Inc., 2021, pp. 155-158. ISBN 978-166543571-0. DOI: <https://doi.org/10.1109/CAS52836.2021.9604170>
- 3) **LUNGU, Ion**, BUSUIOC, Simon, MONAICO, Elena, POTLOG, Tamara. Effect of Particle Size and Roughness on Contact Angle of ZnTe Thin Films. In: *IFMBE Proceedings. 6th International Conference on Nanotechnologies and Biomedical Engineering*. Ediția 6, Vol.91, 20-23 septembrie 2023, Chișinău. Chișinău: Springer Science and Business Media Deutschland GmbH, 2023, pp. 268-277. DOI: https://doi.org/10.1007/978-3-031-42775-6_30
- 4) **LUNGU, Ion**, GHIMPU, Lidia, POTLOG, Tamara. Illumination-Dependent Photovoltaic Parameters of CdS/ZnTe Solar Cells. In: *IFMBE Proceedings. 6th International Conference on Nanotechnologies and Biomedical Engineering*. Ediția 6, Vol.91, 20-23 septembrie 2023, Chișinău. Chișinău: Springer Science and Business Media Deutschland GmbH, 2023, pp. 214-222. DOI: https://doi.org/10.1007/978-3-031-42775-6_24
- 5) GAGARA, Ludmila, **LUNGU, Ion**, GHIMPU, Lidia, POTLOG, Tamara. Synthesis Technology for CdSe/CdTe Heterojunctions and Characterization of Their Photoelectric Properties. In: *IFMBE Proceedings. 6th International Conference on Nanotechnologies and Biomedical Engineering*. Ediția 6, Vol.91, 20-23 septembrie 2023, Chișinău. Chișinău: Springer Science and Business Media Deutschland GmbH, 2023, pp. 206-213. DOI: https://doi.org/10.1007/978-3-031-42775-6_23
- 6) BOTNARIUC, Vasile, GORCEAC, Leonid, COVAL, Andrei, CINIC, Boris, GAUGAȘ, Petru, CHETRUȘ, Petru, **LUNGU, Ion**, RAEVSCHI, Simion. ZnO nanometric layers used in photovoltaic cells. In: *IFMBE Proceedings. 4th International Conference on Nanotechnologies and Biomedical Engineering*. Ediția 4, Vol.77, 18-21 septembrie 2019, Chișinău. Switzerland: Springer Nature Switzerland AG, 2020, pp. 53-56. ISBN 978-303031865-9. DOI: https://doi.org/10.1007/978-3-030-31866-6_11
- 7) POTLOG, Tamara, **LUNGU, Ion**, RAEVSCHI, Simion, BOTNARIUC, Vasile, ROBU, Ștefan, MIMURA, Hidenori. Electrical properties of thermal annealed in vacuum spray deposited al-doped zno thin films. In: *IFMBE Proceedings. 4th International Conference on Nanotechnologies and Biomedical Engineering*. Ediția 4, Vol.77, 18-21 septembrie 2019, Chișinău. Switzerland: Springer Nature Switzerland AG, 2020, pp. 83-87. ISBN 978-303031865-9. DOI: https://doi.org/10.1007/978-3-030-31866-6_18
- 8) QASSEM, Amjad-Al, GAGARA, Ludmila, FEDOROV, Vladimir, **LUNGU, Ion**, POTLOG, Tamara. Comparative study of the P-CDS/N-cdte photovoltaic devices with depleted intrinsic layer. In: *IFMBE Proceedings. 4th International Conference on Nanotechnologies and Biomedical Engineering*. Ediția 4, Vol.77, 18-21 septembrie 2019, Chișinău. Switzerland: Springer Nature Switzerland AG, 2020, pp. 707-711. ISBN 978-303031865-9. DOI: https://doi.org/10.1007/978-3-030-31866-6_125

3.2. in proceedings of scientific events included in other databases accepted by ANACEC

3.3. in proceedings of scientific events included in the Register of materials published based on scientific events organized in the Republic of Moldova

- 1) **LUNGU, Ion**, GADIAC, Ivan. Proprietățile fizice ale straturilor de ZnTe dopate prin imersie în soluție de cupru. In: *Conferința tehnico-științifică a studenților, masteranzilor și doctoranzilor*. Vol.1, 23-25 martie 2021, Chișinău. Chișinău, Republica Moldova: Tehnica-UTM, 2021, pp. 46-49. ISBN 978-9975-45-699-9. https://ibn.idsi.md/vizualizare_articol/133724
- 2) RUSNAC, Dumitru, **LUNGU, Ion**, POTLOG, Tamara. Formarea stării excitate triplet în straturile subțiri dopate cu GA sintetizate din soluție. In: *Integrare prin cercetare și inovare. Științe ale naturii și exacte*. SNE, 10-11 noiembrie 2020, Chișinău. Chisinau, Republica Moldova: CEP USM, 2020, pp. 276-279. ISBN 978-9975-152-50-1. https://ibn.idsi.md/vizualizare_articol/114159
- 3) **LUNGU, Ion**, COLIBABA, Gleb, POTLOG, Tamara. Fabricarea structurilor SnO₂/CdTe/ZnO și cercetarea proprietăților acestora. In: *Integrare prin cercetare și inovare. Științe ale naturii și exacte*. SNE, 10-11 noiembrie 2020, Chișinău. Chisinau, Republica Moldova: CEP USM, 2020, pp. 304-308. ISBN 978-9975-152-50-1. https://ibn.idsi.md/vizualizare_articol/114215
- 4) **LUNGU, Ion**, BOTNARIUC, Vasile, POTLOG, Tamara. Efectul tratării termice în vid asupra structurii și proprietăților optice ale straturilor nanostructurate ZnO dopate cu Ga. In: *Integrare prin cercetare și inovare. Științe ale naturii și exacte*. SNE, 7-8 noiembrie 2019, Chișinău. Chisinau, Republica Moldova: CEP USM, 2019, pp. 234-237. ISBN 978-9975-149-46-4. https://ibn.idsi.md/vizualizare_articol/88887
- 5) GADIAC, Ivan, **LUNGU, Ion**. Rolul hexamethylenetetraminei (HMTA) în sinteza straturilor nanostructurate pe probe de ZnO obținute prin pulverizare cu piroliză. In: *Sesiune națională cu participare internațională de comunicări științifice studențești*. Ediția 24, Vol.1, R, 15 februarie 2020, Chișinău. Chișinău, Republica Moldova: Centrul Editorial-Poligrafic al USM, 2020, pp. 43-46. ISBN 978-9975-142-89-2. https://ibn.idsi.md/vizualizare_articol/102836
- 6) **LUNGU, I.**, GODIAC, I. Influența tratării termice în formarea nanorodurilor de ZnO. In: *Sesiune națională cu participare internațională de comunicări științifice studențești*, Ed. 24, 15 februarie 2020, Chișinău, Republica Moldova: Centrul Editorial-Poligrafic al USM, 2020, Ediția 24, Vol.1, R, pp. 25-28. ISBN 978-9975-45-632-6. https://ibn.idsi.md/vizualizare_articol/106118

4. Patents and other intellectual property objects

4.1. Patents and other intellectual property objects issued by international intellectual property offices (specifying the office)

4.2. Issued by the State Agency for Intellectual Property

5. Other works and achievements specific to various scientific fields (recommended for publication/approved by an authorized institution in the field), such as:

- 1) **LUNGU, I.**, PATRU, R.E., GALCA, A.C., PINTILIE, L., POTLOG, T. DC current-voltage and impedance spectroscopy characterization of CdS/ZnTe heterostructures. In: *Workshop "Application-oriented material development"* September 12-14, 2023, Bucharest, România.
- 2) GAGARA, Ludmila, **LUNGU, Ion**, GHIMPU, Lidia, POTLOG, Tamara. Synthesis Technology for CdSe/CdTe Heterojunctions and Characterization of their Photoelectric Properties. In: *IFMBE Proceedings Nanotechnologies and Biomedical Engineering*. Ediția 6, R, 20-23 septembrie 2023, Chișinău. Chișinău: Springer Science and Business

- Media Deutschland GmbH, 2023, p. 60. ISBN 978-9975-72-773-0. https://ibn.idsi.md/vizualizare_articol/188669
- 3) **LUNGU, Ion**, GHIMPU, Lidia, SUMAN, Victor, UNTILA, Dumitru, POTLOG, Tamara. Illumination-Dependent Photovoltaic Parameters of CdS/ZnTe Solar Cells. In: *IFMBE Proceedings Nanotechnologies and Biomedical Engineering*. Ediția 6, R, 20-23 septembrie 2023, Chișinău. Chișinău: Springer Science and Business Media Deutschland GmbH, 2023, p. 61. ISBN 978-9975-72-773-0. https://ibn.idsi.md/vizualizare_articol/188671
 - 4) **LUNGU, Ion**, BUSUIOC, Simon, MONAICO, Elena, POTLOG, Tamara. Effect of Particle Size and Roughness on Contact Angle of ZnTe Thin Films. In: *IFMBE Proceedings Nanotechnologies and Biomedical Engineering*. Ediția 6, R, 20-23 septembrie 2023, Chișinău. Chișinău: Springer Science and Business Media Deutschland GmbH, 2023, p. 67. ISBN 978-9975-72-773-0.. https://ibn.idsi.md/vizualizare_articol/188685
 - 5) COLIBABA, Gleb, INCULEȚ, Ion, **LUNGU, Ion**. Obtaining of ZnO single crystals with controllable growth direction for application in optoelectronics and photonics. In: *Cercetări și inovații în viziunea tinerilor cercetători "Cadet INOVA'20"*. Nr.5, 26-28 martie 2020, Sibiu. Sibiu, România: Editura Academiei Forțelor Terestre „Nicolae Bălcescu”, 2020, pp. 236-237. https://ibn.idsi.md/vizualizare_articol/116813

ADNOTARE

la teza cu titlul „**FIZICA HETEROSTRUCTURILOR CdS/ZnTe ÎN APLICAȚII FOTOVOLTAICE**”, înaintată de candidatul **Ion LUNGU**, pentru conferirea titlului științific de doctor în științe fizice, la specialitatea **134.01-Fizica și Tehnologia Materialelor**.

Structura tezei: Teza înaintată spre susținere a fost realizată în Laboratorul „Materiale Organice/Anorganice în Optoelectronică” al Universității de Stat din Moldova, Chișinău, 2024. Este scrisă în limba română și constă din introducere, 5 capitole, concluzii generale, recomandări și bibliografie (104 titluri), fiind expusă pe 145 pagini text de bază, 87 figuri și 34 tabele. Rezultatele obținute au fost publicate în 26 lucrări științifice, dintre care un articol în revistă cu impact factor 4,6; 5 articole în reviste din Registrul Național al revistelor de profil; 14 articole în culegeri științifice naționale și internaționale; 5 teze în culegeri științifice naționale și internaționale.

Cuvinte cheie: straturi subțiri, metoda CSS, compuși A^2B^6 , simulare numerică SCAPS-1D, caracteristici J-U, caracteristici C-U, XRD, SEM, AFM, UV-Vis, FL, bandă intermediară, spectroscopia de impedanță.

Domeniul de studiu: Fizica și tehnologia dispozitivelor fotovoltaice pe baza compușilor binari, modelarea numerică a caracteristicilor curent-tensiune și eficienței cuantice externe.

Scopul lucrării constă în analiza potențialului utilizării HJ CdS/ZnTe în aplicații fotovoltaice, cu accent pe elaborarea tehnologiei de obținere a benzii intermediare în stratul absorbant prin încorporarea oxigenului în rețeaua de ZnTe.

Obiectivele cercetării: Conceperea designului optimal al dispozitivului fotovoltaic în baza heterojuncțiunii CdS/ZnTe din punct de vedere al eficienței de conversie a energiei solare în energie electrică prin simularea numerică cu softul SCAPS-1D. Elaborarea tehnologiei de obținere a straturilor subțiri ZnO, CdS, ZnTe prin: dirijarea condițiilor tehnologice, dopare, modificarea controlată a morfologiei, proprietăților cristaline, electrice și optice. Realizarea dispozitivelor fotovoltaice în baza compușilor studiați, cercetarea proprietăților fotoelectrice și stabilirea mecanismului de transport al purtătorilor de sarcină electrică.

Noutatea și originalitatea științifică: Optimizarea parametrilor tehnologici de obținere a straturilor subțiri de ZnTe, utilizând metoda CSS și tratamentul termic în mediu de oxigen la 400 °C, prin studiul structurii, compoziției chimice, absorbției, fotoluminescenței indică formarea benzii intermediare la 1,82 eV, în rezultatul substituției oxigenului cu telur. Realizarea dispozitivelor fotovoltaice cu valoarea tensiunii de circuit deschis de 0,84 V, cu randament de conversie a energiei solare în energie electrică 0,13%, destul de modest, în comparație cu cel obținut prin simulare numerică cu softul SCAPS-1D care indică în funcție de parametrii de intrare: $E_{g(\text{ZnTe})}=2,2$ eV, $E_{g(\text{CdS})}=2,4$ eV, $E_{g(\text{ZnO})}=3,3$ eV, $\chi_{(\text{Ag})}=4,7$ eV următorii parametri fotovoltaici: $U_{CD}=0,89$ V, $J_{SC}=25,9$ mA/cm², $FF=72,6$, $\eta=16,78\%$. Eficiență cuantică internă atinge valoare de aproximativ 0,5 în intervalul lungimilor de undă 490-590 nm. Originalitatea constă în crearea de noi materiale pentru dezvoltarea dispozitivelor fotovoltaice alternative.

Rezultatul/rezultatele obținute care contribuie la soluționarea unei probleme științifice importante: în această teză de doctor a fost propus conceptul de dispozitiv fotovoltaic cu bandă intermediară și elaborate mostre experimentale a dispozitivelor fotovoltaice pe baza HJ CdS/ZnTe.

Semnificația teoretică a lucrării constă în elucidarea proceselor fizico-chimice de formare a benzii intermediare în straturile subțiri de ZnTe obținute, precum și a proceselor de la interfața HJ CdS/ZnTe:O prin analiza caracteristicilor J-U, C-U și a spectroscopiei de impedanță în funcție de temperatura și de frecvență de măsurare.

Valoarea aplicativă: constă în implementarea softului de simulare numerică SCAPS-1D în optimizarea parametrilor fotovoltaici a dispozitivelor fotovoltaice pe baza HJ CdS/ZnTe:O și realizarea experimentală a acestora pentru aplicații în energia verde.

Implementarea rezultatelor științifice: rezultatele științifice obținute pot fi implementate în procesul instructiv-educativ, atât la Facultatea de Fizică și Inginerie a Universității de Stat din Moldova, cât și în alte instituții de învățământ și cercetare din țară și de peste hotare.

ANNOTATION

of the thesis entitled "**PHYSICS OF CdS/ZnTe HETEROSTRUCTURES IN PHOTOVOLTAIC APPLICATIONS**", presented by the candidate **Ion LUNGU**, for obtaining the scientific degree of Doctor in Physical Sciences with specialty **134.01-Physics and Materials Technology**.

Thesis structure: The thesis was performed at the "Organic/Inorganic Materials in Optoelectronics" Laboratory of the State University of Moldova, Chisinau, 2024. It is written in Romanian and consists of an introduction, 5 chapters, general conclusions, recommendations, and bibliography (104 titles). The thesis is presented in 145 pages of basic text, containing 87 figures and 34 tables. The research results have been published in 26 scientific papers, including one journal article with an impact factor of 4.6; 5 articles in magazines from the National Register of professional magazines; 14 articles in national and international scientific collections; 5 theses in national and international scientific collections.

Keywords: thin films, CSS method, A^2B^6 compounds, SCAPS-1D numerical simulation, J-U characteristics, C-U characteristics, XRD, SEM, AFM, UV-Vis, FL, intermediate band, impedance spectroscopy.

Field of study: Physics and technology of photovoltaic devices based on binary compounds, numerical modeling of current-voltage characteristics and external quantum efficiency.

The aim of the work consists of analyzing the potential of using HJ CdS/ZnTe in photovoltaic applications, with an emphasis on the development of the technology to obtain the intermediate band in the absorber layer by incorporating oxygen into the ZnTe network.

Research objectives: Designing the optimal scheme of the photovoltaic device based on the CdS/ZnTe heterojunction in terms of solar energy conversion efficiency through numerical simulation with SCAPS-1D software. The development of the technology for obtaining ZnO, CdS, ZnTe thin films by optimizing the technological conditions, doping for controlled modification of the morphology, crystalline, electrical, and optical properties. Fabrication of photovoltaic devices based on the optimized compounds, studying their photoelectric properties, and establishing the transport mechanism of electric charge carriers.

Scientific novelty and originality of the results: The optimization of the technological parameters for obtaining ZnTe thin films using the CSS method and thermal treatment in an oxygen environment at 400 °C, by studying the structure, chemical composition, absorption, photoluminescence indicates the formation of the intermediate band at 1.82 eV, because of the substitution of oxygen with tellurium. The realization of photovoltaic devices with the open circuit voltage value of 0.84 V, with solar energy conversion efficiency of 0.13%, quite modest, compared to that obtained by numerical simulation with SCAPS-1D software indicating in depending on input parameters: $E_{g(\text{ZnTe})}=2.2$ eV, $E_{g(\text{CdS})}=2.4$ eV, $E_{g(\text{ZnO})}=3.3$ eV, $\chi_{(\text{Ag})}=4.7$ eV following photovoltaic parameters: $V_{OC}=0.89$ V, $J_{SC}=25.9$ mA/cm², FF=72.6, $\eta=16.78\%$. Internal quantum efficiency reaches a value of about 0.5 in the wavelength range 490-590 nm. The originality consists in creating new materials for the development of alternative photovoltaic devices.

The main scientific problem solved: in this PhD thesis, the concept of photovoltaic device with intermediate band was proposed and experimental samples of photovoltaic devices based on HJ CdS/ZnTe were elaborated.

The theoretical significance of the work consists in the elucidation of the physic-chemical processes of the formation of the intermediate band in the ZnTe thin layers obtained, as well as of the processes at the HJ CdS/ZnTe:O interface by analyzing the J-U, C-U characteristics, and impedance spectroscopy as a function of temperature and of measurement frequency.

Applicative value: it consists in the implementation of the numerical simulation software SCAPS-1D in the optimization of the photovoltaic parameters of the photovoltaic devices based on HJ CdS/ZnTe:O and their experimental realization for applications in green energy.

Implementation of scientific results: the obtained scientific results can be implemented in the instructional-educational process, both at the Faculty of Physics and Engineering of the Moldova State University, and in other educational and research institutions from the country and abroad.

АННОТАЦИЯ

Диссертация «**ФИЗИКА ГЕТЕРОСТРУКТУР CdS/ZnTe В ФОТОЭЛЕКТРИЧЕСКИЕ ПРИМЕНЕНИЯ**», представленной **Лунгу Ион**, на соискание степени доктора физических наук по специальности **134.01-Физика и технология материалов**.

Структура диссертации: Представленная на защиту диссертация выполнена в лаборатории «Органические/Неорганические Материалы в Оптоэлектронике» Государственного университета Молдовы, Кишинев, 2024. Она написана на румынском языке и состоит из введения, 5 глав, общих выводов, рекомендаций и библиографии (104 наименований), содержит 145 страниц основного текста, 87 рисунка и 34 таблиц. Полученные результаты опубликованы в 26 научных работах, в том числе одна журнальная статья с импакт-фактором 4,6; 5 статей в журналах Национального реестра профессиональных журналов; 14 статей в национальных и международных научных сборниках; 5 диссертаций в национальных и международных научных сборниках.

Ключевые слова: тонкие пленки, метод квазизамкнутого объема, соединения A^2B^6 , I-U характеристики, C-U характеристики, РФА, СЭМ, АСМ, УФ-Вид, ФЛ, промежуточная зона, импедансная спектроскопия, численное моделирование.

Область научных интересов: Физика и технология фотоэлектрических устройств на основе бинарных соединений, численное моделирование вольтамперных характеристик и внешнего квантового выхода.

Цель работы состоит в анализе потенциала использования НГ CdS/ZnTe в фотоэлектрических устройствах с упором на разработку технологии получения промежуточной полосы в абсорбирующем слое путем внедрения кислорода в решетку ZnTe.

Задачи работы: Разработка оптимально дизайна фотоэлектрического устройства на основе гетероперехода CdS/ZnTe с точки зрения эффективности преобразования солнечной энергии путем численного моделирования в программе SCAPS-1D. Разработка технологии получения тонких слоев ZnO, CdS, ZnTe путем: управление технологических условий, легирования, контролируемого изменения морфологии, кристаллических, электрических и оптических свойств. Создание фотоэлектрических устройств на основе изученных соединений, исследование фотоэлектрических свойств и установление механизма переноса носителей электрического заряда.

Научная новизна и оригинальность: Оптимизация технологических параметров *при* различных условиях *получения* тонких слоев ZnTe методом CSS и термической обработкой в кислородной среде при температуре 400 °С, путем изучения структуры, химического состава, поглощения, фотолуминесценции указывает на образование промежуточной полосы при 1,82 эВ в результате замещения теллура кислородом. Реализация фотоэлектрических устройств со значением напряжения холостого хода 0,84 В, с КПД преобразования солнечной энергии 0,13%, достаточно скромным по сравнению с полученным при численном моделировании в программе SCAPS-1D с указанием в зависимости от входных параметров: $E_{g(ZnTe)}=2,2$ эВ, $E_{g(CdS)}=2,4$ эВ, $E_{g(ZnO)}=3,3$ эВ, $\chi_{(Ag)}=4,7$ эВ следующие фотоэлектрические параметры: $B_{XX}=0,89$ В, $J_{SC}=25,9$ мА/см², FF=72,6, $\eta=16,78$ %. Внутренний квантовый выход достигает значения около 0,5 в диапазоне длин волн 490-590 нм. Оригинальность состоит в создании новых материалов для развития альтернативных фотовольтаических приборов.

Решенная основная научная задача: в данной докторской диссертации была предложена концепция фотоэлектрического устройства с промежуточной зоной и разработаны экспериментальные образцы фотоэлектрических устройств на основе НГ CdS/ZnTe.

Теоретическая значимость работы состоит в выяснении физико-химических процессов формирования промежуточной зоны в полученных тонких слоях ZnTe, а также процессов на границе раздела НГ CdS/ZnTe:О путем анализа J-U, C-U характеристик и импеданса спектроскопии в зависимости от температуры и частоты измерения.

Прикладное значение: заключается во внедрении программы численного моделирования SCAPS-1D при оптимизации фотоэлектрических параметров фотоэлектрических устройств на основе НГ CdS/ZnTe:О и их экспериментальной реализации для приложений в зеленой энергетике.

Внедрение научных результатов: полученные научные результаты могут быть внедрены в учебно-образовательный процесс, как на физико-техническом факультете Государственного университета Молдовы, так и в других образовательных и научно-исследовательских учреждениях в стране и за рубежом.

LUNGU Ion

**PHYSICS OF CdS/ZnTe HETEROSTRUCTURES IN
PHOTOVOLTAIC APPLICATIONS**

134.01 Physics and Materials Technology

Abstract of the PhD thesis

Approved for printing: 23.08.2024
Offset paper. Offset printing.
Print Sheets: 2.0

Paper size: 60×84 1/16
Print run: **20ex.**
Order no. 57

„Ion Creangă” SPU Editorial-Polygraphic Center
1, Ion Creanga str., Chisinau, MD-2069